Atmospheric
Chemistry
and Physics
Discussions

Open Access

Free troposphere ozone and carbon monoxide over the North Atlantic for 2001–2011

A. Kumar[1], S. Wu[1,2], M. F. Weise[1,*], R. Honrath[1,†], R. C. Owen[3], D. Helmig[4], L. Kramer[2], M. Val Martin[5], and Q. Li[6]

[1]Department of Civil & Environmental Engineering, Michigan Technological University, Houghton, Michigan, USA
[2]Department of Geological and Mining Engineering and Sciences, Michigan Technological University, Houghton, Michigan, USA
[3]US EPA, Research Triangle Park, North Carolina, USA
[4]Institute of Alpine and Arctic Research, University of Colorado at Boulder, Boulder, Colorado, USA
[5]Department of Atmospheric Sciences, Colorado State University, Fort Collins, Colorado, USA
[6]Department of Atmospheric & Oceanic Sciences, University of California Los Angeles, Los Angeles, California, USA
[*]now at: ARCADIS, Novi, Michigan, USA
[†]deceased

Discussion Paper | Discussion Paper | Discussion Paper | Discussion Paper

ACPD
13, 15377–15407, 2013

Free troposphere ozone and carbon monoxide over the North Atlantic

A. Kumar et al.

Title Page

Abstract | Introduction

Conclusions | References

Tables | Figures

◄◄ | ►►

◄ | ►

Back | Close

Full Screen / Esc

Printer-friendly Version

Interactive Discussion

Free troposphere ozone and carbon monoxide over the North Atlantic

A. Kumar et al.

Title Page

Abstract	Introduction
Conclusions	References
Tables	Figures

|◄ | ►|

◄ | ►

Back | Close

Full Screen / Esc

Printer-friendly Version

Interactive Discussion

Abstract

In-situ measurements of carbon monoxide (CO) and ozone (O_3) at the Pico Mountain Observatory (PMO) located in the Azores, Portugal are analyzed together with results from atmospheric chemical transport modeling (GEOS-Chem) and satellite remote sensing (AIRS for CO and TES for O_3) to examine the evolution of free-troposphere CO and O_3 over the North Atlantic for 2001–2011. GEOS-Chem captured the seasonal cycles for CO and O_3 well but significantly underestimated the mixing ratios of CO, particularly in spring. Statistically significant (using a significance level of 0.05) decreasing trends were found for both CO and O_3 based on harmonic regression analysis of the measurement data. The best estimates of the trend for CO and O_3 measurements are -0.31 ± 0.30 (2-σ) ppbv yr^{-1} and -0.21 ± 0.11 (2-σ) ppbv yr^{-1}, respectively. Similar decreasing trends for both species were obtained with GEOS-Chem simulation results. The major factor contributing to the reported decrease in CO and O_3 mixing ratios at PMO over the past decade is the decline in anthropogenic CO and O_3-precursor emissions in regions such as North America and Europe. The increase in Asian emissions does not seem to outweigh the impact of these declines resulting in overall decreasing trends for both CO and O_3. For O_3, however, increase in atmospheric water vapor content associated with climate change also appears to be a contributing factor causing enhanced destruction of the O_3 during transport from source regions. These hypotheses are supported by results from the GEOS-Chem tagged CO and tagged O_3 simulations.

1 Introduction

Carbon monoxide (CO) and ozone (O_3) are important atmospheric pollutants in the troposphere (Seinfield and Pandis, 2006). The major sources of atmospheric CO include incomplete combustion of fossil fuels (Holloway et al., 2000; Khalil and Rasmussen, 1994; Seinfeld and Pandis, 2006) and biomass burning. CO is also formed through

the oxidation of volatile organic compounds (VOCs) by the hydroxyl radical (OH). O_3 is formed in the troposphere through photochemical reactions in the presence of O_3 precursors which include the nitrogen oxides ($NO + NO_2 = NO_x$), CO and VOCs. The dominant loss pathway for tropospheric O_3 is photolysis followed by reaction with water vapor.

Atmospheric transport across the North Atlantic Ocean carries air pollutants from the continent of North America towards Europe. CO has a chemical lifetime of several months (Seinfeld and Pandis, 2006) and the lifetime for O_3 is 2–4 weeks in the troposphere (Law, 2010). These relatively long lifetimes enable these species to undergo intercontinental transport. Thus, changes in emissions from source regions (such as North America) can have significant implications for atmospheric composition in downwind regions such as North Atlantic or Europe. Li et al. (2002) found that 20 % of summer violations of O_3 air quality standards in Europe would not have occurred in the absence of North American anthropogenic emissions.

Increases in anthropogenic emissions of NO_x, CO and VOCs have led to increases in free tropospheric O_3 since pre-industrial times (Wang et al., 1998) although several studies have reported divergent trends of tropospheric O_3 over different regions of the Northern Hemisphere (Brunke et al., 1998; Fusco and Logan, 2003; Guicherit and Roemer, 2000; Jaffe et al., 2003; Lee et al., 1998; Oltmans et al., 2006). Over the past decade, emissions of O_3 precursors have declined significantly in North America and Europe, while those in Asia have increased (Hudman et al., 2009; Vingarzan, 2004). Figure 1 shows the trends of anthropogenic emissions of CO and NO_x in the United States (US) from 2000–2011. US sources account for approximately 80 % of anthropogenic emissions from North America (Wang et al., 2009). These changes in emissions are expected to influence the free troposphere CO and O_3 concentrations over the North Atlantic. The Pico Mountain Observatory located in the central North Atlantic region (details provided in the next section) is a unique site that can be used to measure species relevant to long range transport and thereby examine the direct continental outflow from North America. In this study, we combine analyses of the

Free troposphere ozone and carbon monoxide over the North Atlantic

A. Kumar et al.

Title Page

Abstract	Introduction
Conclusions	References
Tables	Figures

◀◀ ▶▶

◀ ▶

Back Close

Full Screen / Esc

Printer-friendly Version

Interactive Discussion

continuous in-situ measurements of CO and O_3 at this station and results from the Goddard Earth Observing System chemical (GEOS-Chem) transport model to examine the trends in free-tropospheric CO and O_3 over the North Atlantic for the past decade.

2 Measurement data

2.1 Measurements at the Pico Mountain Observatory

The Pico Mountain Observatory (PMO, formerly called PICO-NARE) is located on the summit of Pico Mountain on the Pico island in the Azores, Portugal (38° 28′ N, 28° 24′ W) at an altitude of 2225 m (Honrath et al., 2004). The station during most times receives air characteristic of the lower free troposphere (FT) and is well above the Marine Boundary Layer (MBL) during summertime. The island population is low (around 15 000) and is concentrated near sea level which results in the site having negligible anthropogenic influence on the free troposphere composition, although upslope flows have been found to occur resulting in the transport of low-altitude air to the mountaintop (Kleissl et al., 2007). However, the occurrence of such flow is not very frequent and even when it occurs it was found that the air did not originate from the surface (Kleissl et al., 2007).

The station is also frequently impacted by export of North American pollution during summertime and outflow from arctic and subarctic regions resulting in transport of biomass burning emissions from Canada, Alaska and Siberia (Honrath et al., 2004; Val Martin et al., 2008a). Val Martin et al. (2006) reported that North American boreal wildfires contributed significantly to enhancements in CO and O_3 background mixing ratios during the summer of 2004. Honrath et al. (2004) observed frequent enhancements in CO levels above the marine background levels during the summertime in 2001–2003 which they attributed to North American pollution outflow or long-range transport of biomass burning emissions. High levels of both CO and O_3 were observed during the periods of biomass burning.

Free troposphere ozone and carbon monoxide over the North Atlantic

A. Kumar et al.

Title Page

Abstract | Introduction

Conclusions | References

Tables | Figures

◄ | ►

◄ | ►

Back | Close

Full Screen / Esc

Printer-friendly Version

Interactive Discussion

CO and O_3 have been measured at PMO using instruments described in Honrath et al. (2004). We use hourly CO data covering 2001–2010 and O_3 data spanning 2001–2011 with most of the available data spanning May–September. Only days with full 24 h data availability were used to calculate the daily average mixing ratios of CO and O_3. These data account for approximately 76 % (87 %) of the total CO (O_3) measurements available from the station.

2.2 AIRS/AQUA data for CO

The Atmospheric Infrared Sounder (AIRS) was launched onboard the AQUA satellite on 4 May 2002. It is a polar orbiting nadir-viewing thermal IR sounder with cloud clearing capability and retrieves CO at 4.7 microns with 70 % daily global coverage; 100 % between 45° and 80° longitude (McMillan et al., 2005; Yurganov et al., 2008). We use AIRS level 3 version 5 monthly data obtained from Giovanni, Goddard Earth Sciences Data and Information Services Center (GES DISC). Data are available at http://disc.sci.gsfc.nasa.gov/giovanni#instances (Acker and Leptoukh, 2007). Level 3 datasets have undergone rigorous processing and are available with no subsequent processing required. As done in prior studies, AIRS measurements with more than 0.5 degrees of freedom (Fisher et al., 2010) were included in the analysis. Previous comparisons of AIRS with in-situ measurements reveal a positive bias of $\sim$ 10 % in the Northern Hemisphere (Fisher et al., 2010; Kopacz et al., 2010). Retrievals for the area matching the same horizontal grid as GEOS-Chem over PMO (32.5 to 27.5° W and 36 to 40° N) centered at 802 hPa (roughly 2.2 km, the same elevation as PMO) are used in this study. Since both the measurement data at PMO and GEOS-Chem use both day and night values, day and night retrievals are used for AIRS as well.

2.3 TES/Aura data for O_3

The Tropospheric Emission Spectrometer (TES) was launched in July 2004 aboard the EOS Aura satellite. Data were obtained from Giovanni online data system, developed

and maintained by the NASA GES DISC as mentioned above (Sect. 2.2). TES is nadir viewing in a polar orbiting sun synchronous orbit on the same track as AIRS/Aqua with a local crossing time of 01:45 and 13:45 (Zhang et al., 2010). We use available data for the period covering 2005–2010 in this study. The data for 2008–2009 were not available. The level three data used were pre-processed and all negative values were filtered out. Previous comparisons with in-situ measurements show that TES has a positive bias of 5.3 ppbv for O_3 at 500 hPa (Zhang et al., 2010).

3 Model description

We use GEOS-Chem, a global three-dimensional model of tropospheric chemistry driven by assimilated meteorological observations from the Goddard Earth Observing System (GEOS) of the NASA Global Modeling Assimilation Office (Bey et al., 2001; Fairlie et al., 2007; Evans and Jacob, 2005; Martin et al., 2002; Park et al., 2004) to simulate the evolution of atmospheric composition in the past decade. The model has fully coupled O_3–NO_x–VOC-aerosol chemistry and has been extensively evaluated and applied to a wide range of research topics related to atmospheric chemistry and air quality (e.g., Duncan et al., 2007; Evans and Jacob, 2005; Martin et al., 2002; Park et al., 2004; Wu et al., 2007). There have been different versions of the GEOS meteorology including GEOS-3, GEOS-4 and GEOS-5 with each spanning different periods. GEOS-5 is the latest version covering the period 2004–2011. Available horizontal grid resolutions in the model range from $4° \times 5°$ to $0.5° \times 0.667°$ (latitude × longitude). Emission inventories in GEOS-Chem cover various sources including anthropogenic, biomass burning, biofuel and biogenic emissions. Anthropogenic emissions follow the Emissions Database for Global Atmospheric Research (EDGAR) global inventory (Olivier and Berdowski, 2001) and are updated with regional inventories including the US EPA National Emissions Inventory (EPA/NEI05 and EPA/NEI99), the Environment Canada National Pollutant Release (CAC) Inventory, the European Monitoring and Evaluation Program (EMEP) Inventory, the Streets Emissions Inventory in Asia (Streets et al.,

Free troposphere ozone and carbon monoxide over the North Atlantic

A. Kumar et al.

2003, 2006; Zhang et al., 2009) and the Big Bend Regional Aerosol and Visibility Observational (BRAVO) study emissions inventory for Mexico and some neighboring US states. The biomass burning emissions follow either the Global Fire Emissions Database (GFED) v2 (1997–2008) (Van Der Werf et al., 2006) or GFEDv3 (1997–2010) monthly inventories (Van Der Werf et al., 2010) and biogenic VOC emissions are taken from the Model of Emissions of Gases and Aerosols from Nature (MEGAN) global inventory. Emissions from other natural sources (e.g. lightning, volcanoes) are also included. For chemistry, either the Kinetic Pre-Processor (KPP) (Eller et al., 2009; Sandu and Sander, 2006) or the SPARSE MATRIX VECTORIZED GEAR 2 (SMVGEAR 2) (Eller et al., 2009) chemistry solver can be used. The Linearized Ozone (LINOZ) mechanism (McLinden et al., 2000) is used for the stratosphere-troposphere exchange of O_3.

In addition to the standard full chemistry simulations with GEOS-Chem, we also carry out special tagged simulations (tagged CO and tagged O_3 simulations) to better identify the contributions to CO and O_3 at PMO from various source regions. A brief description of the simulations used in this study and the archived data is provided in the following sections.

3.1 Full chemistry simulations used

The full chemistry simulations using the standard version of GEOS-Chem (with the SMVGEAR 2 chemical solver) with normal emissions are referred here as FCNE simulations. We used the $4° \times 5°$ (latitude × longitude) horizontal resolution and a one year spin up for all the FCNE simulations. GEOS-4 meteorology fields were used for 2001–2004 whereas those from GEOS-5 version covered the period from 2005 onwards. Regional emission inventories for anthropogenic (fossil fuel and biofuel) emissions were used over Canada (CAC inventory), Mexico (BRAVO), Asia (Streets), USA (NEI2005 and EPA/NEI99) and Europe (EMEP). The other regions were covered by the EDGAR global anthropogenic emissions inventory. Biogenic VOCs in the model include emissions of isoprene, methyl butenol and seven monoterpene compounds following the

MEGAN scheme (Guenther et al., 2006). For biomass burning emissions, the GFEDv2 monthly inventory was used (as the GFEDv3 inventory was not available with the model version (v8-03-01) used). Model simulated CO and O_3 mixing ratios for the grid box covering PMO were archived with a 4 h temporal resolution.

5   Table 1 summarizes the anthropogenic and biomass burning CO emissions in GEOS-Chem for various regions of the Northern Hemisphere for 2001–2009. The model shows significant declines in anthropogenic CO for North America and Europe but increases from Asia during this time period.

A sensitivity run was also performed to assess the impact of North American fossil
10   fuel combustion on CO and O_3 at PMO by excluding those emissions. This run had no fossil fuel emissions for the region covering the US, Canada and Mexico (15 to 88° N (latitude) and 50 to 165° W (longitude)).

3.2   Tagged CO simulation

The GEOS-Chem tagged CO simulation was used to determine the contribution to CO
15   mixing ratios at PMO from various geographical regions (e.g. Asia, North America) and sources (e.g. biomass burning, biofuels). It is one of the several offline simulations included in GEOS-Chem and consists of source/region-specific CO tracers. The CO sources accounted for include fossil fuels, biofuels, biomass burning, anthropogenic and biogenic VOCs. A detailed description can be found in Duncan et al. (2007). The
20   reaction of CO with OH is the only sink considered. We used v9-01-02 of the model with the $4° \times 5°$ (latitude × longitude) horizontal resolution. For this simulation, emission inventories included to account for anthropogenic CO production were the global EDGAR inventory, CAC inventory over Canada, BRAVO over Mexico, EPA/NEI99 over North America, Streets over South-East Asia and the RETRO (for global anthropogenic
25   VOCs) inventory. For biomass burning emissions, the monthly GFEDv3 emissions (available with the version used) were used. The OH concentrations used were those archived from a separate full chemistry simulation. Restart files for the tagged CO simulation were generated by an eleven month (February–December 2000) spin up (with

zero initial concentrations for all the tracers) for the period 2001–2004 (using GEOS-4) until steady state concentrations were reached. For the run with GEOS-5 (2005–2010), a one year spin up (January–December 2004) was used. The data archived consists of the time-series of 4 hourly instantaneous values of all the CO tracers at PMO from 2001–2010.

3.3 Tagged O_3 simulation

The tagged O_3 simulation was used to attribute the O_3 mixing ratios at PMO to O_3 production from various regions. It uses chemical production/loss rates of O_3 archived from the FCNE simulation. We used version 09-01-02 of GEOS-Chem (horizontal resolution $4° \times 5°$ (latitude × longitude)) for this simulation and the same version was also used to archive the O_3 production/loss rates from 2000–2011. Restart files were generated in the same manner as for the tagged CO simulation. The time-series of 4 hourly instantaneous values of all the tracers was archived from 2001–2011 for the location and altitude corresponding to PMO.

4   Seasonal variation of CO and O_3 at PMO

The box plot in Fig. 2 shows the seasonal variation of CO and O_3 at PMO from ground-based in situ measurements, satellite retrievals and GEOS-Chem model simulations. Daily (24 h) average values for CO and O_3 from the whole-year period of September 2004 to August 2005 were used to construct the box plot as this period has the best data availability for the measurements. Both CO and O_3 show maxima in the spring-time and minima in the summer-time, which is consistent with the model results and measurement data. Similar seasonal variations have also been reported for these species at other remote sites such as Mace Head (Derwent et al., 1998) and mountaintop stations such as Mt. Cimone (Bonasoni et al., 2000), and for CO in a previous study at the PMO (Val Martin et al., 2008b). However, GEOS-Chem significantly

underestimates the mixing ratios of CO (by 20–30 ppbv) throughout the year which possibly reflects some low biases in the CO emission inventories. The underestimation of CO by the model has been reported by previous studies (Bey et al., 2001; Duncan and Logan, 2008; Duncan et al., 2007; Val Martin et al., 2008b) as well. In contrast, GEOS-Chem reproduces both the seasonal variation and magnitude of O_3 very well.

5   General long term trends of CO and O_3 at PMO

5.1   Trend analysis methodology

Two-sided parametric hypothesis testing (null hypothesis of no trend and alternate hypothesis of non-zero trend) was used to analyze the trends in CO and O_3 mixing ratios at PMO for 2001–2011. We employed a multiple regression model that is similar to the additive model of a time-series and contains sinusoidal functions to represent the characteristic seasonal variations of both CO and O_3. The sinusoidal functions use a time period of one year to reflect the seasonal variations of CO and O_3. A linear term in time was used to represent the long term trend in CO or O_3. Following Helsel and Hirsch (2002), we express the model for daily average values of CO or O_3 as:

$$C_t = a_0 + a_1 t + a_2 \sin\left(\frac{2\pi t}{365}\right) + a_3 \cos\left(\frac{2\pi t}{365}\right) + \varepsilon_t \tag{1}$$

Where:
C_t: Mixing ratio of the species at a time t (in days of year) (time being measured from a reference year (1 January 1900 in this case))
a_0, a_1, a_2, a_3: regression coefficients
ε_t: residual from the model

For all datasets consisting of daily averages, a five day centered simple moving average scheme was applied to the data before fitting the regression model. Coefficients

in the regression equation were determined by the least squares method and the statistical significance of the t statistic corresponding to the slope term was examined by comparing the probability of observing a t statistic of same or greater magnitude with the null hypothesis being true (p value) with the significance level α (0.05 used for this study).

5.2 Trends obtained from PMO data and GEOS-Chem results

The regression model in Eq. (1) was applied to the time-series of CO and O_3 (for both the in-situ measurements and GEOS-Chem FCNE simulation output) at PMO. Table 2 lists the trends for both the measurement data and GEOS-Chem output along with the associated p values. Figure 3 shows the regression fits for the CO and O_3 measurements and Fig. 4 contains the fits for the modeled (GEOS-Chem FCNE simulation) CO and O_3. The observations show statistically significant decreasing trends for both the species over the study period with CO showing a decrease of -0.31 ± 0.30 (2-σ) ppbv yr^{-1} (p value $= 0.04$) and O_3 decreasing by -0.21 ± 0.11 (2-σ) ppbv yr^{-1} (p value < 0.001). GEOS-Chem also shows statistically significant decreasing trends for both CO (-0.34 ± 0.08 (2-σ) ppbv yr^{-1}, p value < 0.001) and O_3 (-0.53 ± 0.04 (2-σ) ppbv yr^{-1}, p value < 0.001).

These decreasing trends are in agreement with those obtained from observation data at other stations in the North Atlantic such as Tudor Hill, Bermuda (TH) and Mace Head, Ireland (MH) (data available at http://ds.data.jma.go.jp/gmd/wdcgg/cgi-bin/wdcgg/catalogue.cgi). For TH, the harmonic regression analysis of O_3 mixing ratios from 2003–2011 yields a statistically significant decreasing trend (p value < 0.001) of 1.1 ± 0.11 (2-σ) ppbv yr^{-1}, whereas CO at MH (2001–2011) shows a statistically significant decreasing trend (-1.4 ± 0.20 (2-σ) ppbv yr^{-1}, p value < 0.001) as well. However, measurements at Izana, Tenerife (IT) (data available at http://ds.data.jma.go.jp/gmd/wdcgg/cgi-bin/wdcgg/catalogue.cgi) show an increasing trend of 0.10 ± 0.07 (2-σ) ppbv yr^{-1} for O_3 over the study period. This opposite trend at IT could indicate

the fact that it is further south and less affected by the continental outflow from North America.

Previous studies such as Lelieveld et al. (2004) and Derwent et al. (2007) have reported upward trends in O_3 over the North Atlantic for the periods 1977–2002 and 1987–2007, respectively. The discrepancy appears largely due to the different time frame used in these studies. This factor is exemplified by the different trends observed for O_3 at TH (increasing trend of 0.70 ± 0.10 (2-σ) ppbv yr^{-1}, p value < 0.001) for the earlier decade of 1988–1998 as compared to the decreasing trend for 2003–2011.

One of the major factors that could lead to a decrease in CO and O_3 mixing ratios over the North Atlantic is the decline in anthropogenic emissions from North America (of which 80 % emissions are from the US) in the past decade. The trends for US anthropogenic emissions of CO and NO_x are shown in Fig. 1. In order to investigate this hypothesis we first carried out sensitivity runs by turning off North American fossil fuel emissions in the model (Sect. 3.1) to derive the contribution of North American anthropogenic emissions to CO and O_3 at PMO. Our results show that the anthropogenic emissions from North America enhance the annual means of CO and O_3 at PMO by 8.6 and 4.0 ppbv yr^{-1}, respectively (Table 3). Also, Fig. 1 shows that the US CO emissions have declined approximately by a factor of 1/3 and assuming a linear correspondence between the US emissions and their contribution to CO mixing ratios at PMO, this would amount to a decrease of approximately 2.9 ppbv in the CO at the station (over the past decade). This change is similar to that obtained from the harmonic regression analysis of CO measurements at PMO, suggesting that the decline in the CO at the station correlates particularly well with the US emission declines. For CO, the largest contribution from North American emissions was found in the winter and spring, which reflects stronger atmospheric transport and longer chemical lifetimes of CO (due to low levels of OH) during those seasons, as previously noted by (Val Martin et al., 2008b). In contrast, for O_3, the least North American contribution was found during winter reflecting the NO_x-saturated regime where O_3 production is more sensitive

Title Page

Abstract | Introduction

Conclusions | References

Tables | Figures

◄ | ►

◄ | ►

Back | Close

Full Screen / Esc

Printer-friendly Version

Interactive Discussion

to the photochemically generated hydrogen oxide radicals (HO_x) (Jacob et al., 1995; Kleinman et al., 1995).

In order to better understand and quantify the effects associated with the decreases in North American emissions, we also carried out tagged CO and O_3 simulations with the GEOS-Chem model. Results of the trend analysis for the tagged CO simulation are summarized in Table 4. The contribution of CO produced from anthropogenic fossil fuel emissions in the US to CO at PMO shows a statistically significant (p value < 0.001) decrease over the study period. The contribution of biomass burning emissions in Europe also shows a statistically significant (p value < 0.001) decrease. On the other hand, contribution of fossil fuel emissions in Asia shows a statistically significant (p value < 0.001) increase. These results indicate that reductions in CO from North America and Europe are the primary reasons for the decreasing CO at PMO, which outweigh the effects of increasing CO from Asia in the past decade.

Table 5 summarizes the results of the statistical analysis for the tagged O_3 simulation. Statistically significant (p value < 0.001) decreasing trends are obtained for the contributions to O_3 at PMO from O_3 production in the boundary layer over various regions including North America, Europe and Asia. The contribution of O_3 production in the middle troposphere (MT) (Boundary Layer top – 350 hPa) also shows a decreasing trend (p value < 0.001) over the study period. On the other hand, an increasing trend (p value < 0.001) was identified for the contribution from O_3 produced in the upper troposphere (UT) (350 hPa – tropopause).

The decreasing trends for contributions to O_3 at PMO from North America and Europe are consistent with the declines in anthropogenic O_3 precursor emissions in these regions. On the other hand, the decrease in the contribution of O_3 produced in Asia (where anthropogenic precursor emissions have been increasing) may reflect the impacts from climate change in the past decade. Except for regions with strong emissions of O_3 precursors, climate change generally decreases surface O_3 due to enhanced O_3 destruction associated with higher water vapor concentration in the atmosphere (e.g., Johnson et al., 1999; Wu et al., 2008). With reduced chemical lifetime of O_3, this effect

Title Page

Abstract | Introduction

Conclusions | References

Tables | Figures

|◄ | ►|

◄ | ►

Back | Close

Full Screen / Esc

Printer-friendly Version

Interactive Discussion

is particularly important for remote regions and the long range transport of atmospheric O_3. Analysis of the atmospheric water vapor concentrations in the past decade shows significant increases (up to 20 %) over the North Atlantic for the study period which contributes to a shorter O_3 lifetime during transport. The increase in the contribution of O_3 produced in the UT could be due to an increase in the NO_x production from lightning. The upper troposphere O_3 is highly sensitive to NO_x emissions from lightning, with the O_3 production efficiency (referenced to NO_x emissions) about six times higher than that for NO_x emissions in surface air (Wu et al., 2008). The statistically significant decreasing trend for the contribution of O_3 production in the North Atlantic largely reflects the decline in the anthropogenic emissions from North America. When comparing the contributions from various regions (North America, Europe and Asia) in Table 5, we can see that the reductions in anthropogenic emissions of O_3 precursors is the most important factor contributing to the decrease in O_3 mixing ratios observed at PMO.

6   Conclusions and summary

This study analyzes in-situ measurements of CO and O_3 at the Pico mountaintop observatory and output from GEOS-Chem model simulations to determine the trends in CO and O_3 over the North Atlantic region for the past decade. The GEOS-Chem model performance is also evaluated by comparing simulation results against measurements at PMO and satellite output. The model reproduces the seasonal variations of CO and O_3 at PMO reasonably well although it significantly underestimates CO at this remote site.

Sensitivity studies show that North American fossil fuel emissions account for 8.6 and 4.0 ppbv CO and O_3, respectively, of the total mixing ratios observed at PMO. This contribution to the CO mixing ratios is greatest during winter and spring, reflecting the longer CO lifetimes and stronger transport during those seasons. In contrast,

the contribution to the O_3 is found to be smallest during winter reflecting the low O_3 production and low sensitivity to NO_x emissions during wintertime.

Harmonic regression analysis of the observed CO and O_3 mixing ratios at PMO for 2001–2011 shows statistically significant (with p values of 0.04 and 0.0001, respectively) decreases for both species. The best estimates of the trends for the CO and O_3 measurements are -0.31 ± 0.30 (2-σ) ppbv yr^{-1} and -0.21 ± 0.11 (2-σ) ppbv yr^{-1}, respectively. GEOS-Chem model simulations for the past decade also yield decreasing trends for CO and O_3 at PMO. We conducted tagged simulations for CO and O_3 respectively with GEOS-Chem to attribute these decreases. Contribution to CO at PMO from fossil fuel emissions in the United States shows a statistically significant (p value < 0.001) decreasing trend (-0.27 ± 0.05 (2-σ) ppbv yr^{-1}) while the contribution from fossil fuel emissions in Asia shows a statistically significant (p value < 0.001) increasing trend ($+0.35 \pm 0.03$ (2-σ) ppbv yr^{-1}). Also, biomass burning emissions in Europe show statistically significant (p value < 0.001) decreasing contribution (-0.3 ± 0.03 (2-σ) ppbv yr^{-1}). These results indicate that even though the increasing CO emissions from Asia in the past decade have led to increasing enhancement in CO over the North Atlantic, the decreases in CO from North America and Europe more than compensate these increases and result in an overall decrease in CO mixing ratios at PMO. The changes in O_3 at PMO are attributed to O_3 production in various regions (e.g., North America, North Atlantic, Europe and Asia) through tagged O_3 simulations with the GEOS-Chem model. Contributions from O_3 produced in the lower and middle troposphere also show statistically significant decreasing trends. The decreases in the contribution of O_3 from North America and Europe as well as the North Atlantic are consistent with the decreases in anthropogenic emissions of O_3 precursors in North America and Europe in the past decade. While the anthropogenic emissions in Asia have increased in the past decade, the decreasing trend for contribution to PMO O_3 from Asia possibly reflects the impacts of climate change which is expected to enhance the destruction (in particular for remote regions) and therefore reduce the long-range transport of O_3. Overall, the emission reduction of O_3 precursors in North America in

the past decade is the most important factor contributing to the observed decreasing trends of CO and O_3 at PMO.

References

Acker, J. G. and Leptoukh, G.: Online analysis enhances use of NASA Earth science data, EOS, Transactions American Geophysical Union, 88, 14–17, doi:10.1029/2007EO020003, 2007.

Bey, I., Jacob, D. J., Yantosca, R. M., Logan, J. A., Field, B. D., Fiore, A. M., Li, Q., Liu, H. Y., Mickley, L. J., and Schultz, M. G.: Global modeling of tropospheric chemistry with assimilated meteorology: Model description and evaluation, J. Geophys. Res., 106, 23073–23096, 2001.

Bonasoni, P., Stohl, A., Cristofanelli, P., Calzolari, F., Colombo, T., and Evangelisti, F.: Background ozone variations at Mt. Cimone station, Atmos. Environ., 34, 5183–5189, 2000.

Brunke, E., Meyer, Ñ., Lathrop, J., Johnson, B., Shadwick, D., Cuevas, E., Schmidlin, F., Tarasick, D., Claude, H., and Kerr, J.: Trends of ozone in the troposphere, Geophys. Res. Lett., 25, 139–142, 1998.

Derwent, R. G., Simmonds, P. G., Scuring, S., and Dimmer, C.: Observation and interpretation of seasonal cycles in the surface concentrations of ozone and carbon monoxide at Mace Head, Ireland, from 1990 to 1994, Atmos. Environ., 32, 145–157, 1998.

Derwent, R. G., Simmonds, P. G., Manning, A. J., and Spain, T. G.: Trends over a 20-year period from 1987 to 2007 in surface ozone at the atmospheric research station, Mace Head, Ireland, Atmos. Environ., 41, 9091–9098, 2007.

Duncan, B. N. and Logan, J. A.: Model analysis of the factors regulating the trends and variability of carbon monoxide between 1988 and 1997, Atmos. Chem. Phys., 8, 7389–7403, doi:10.5194/acp-8-7389-2008, 2008.

Duncan, B. N., Logan, J. A., Bey, I., Megretskaia, I. A., Yantosca, R. M., Novelli, P. C., Jones, N. B., and Rinsland, C. P.: Global budget of CO, 1988–1997: Source estimates and validation with a global model, J. Geophys. Res., 112, D22301, doi:10.1029/2007JD008459, 2007.

Eller, P., Singh, K., Sandu, A., Bowman, K., Henze, D. K., and Lee, M.: Implementation and evaluation of an array of chemical solvers in the Global Chemical Transport Model GEOS-Chem, Geosci. Model Dev., 2, 89–96, doi:10.5194/gmd-2-89-2009, 2009.

Evans, M. J. and Jacob, D. J.: Impact of new laboratory studies of N_2O_5 hydrolysis on global model budgets of tropospheric nitrogen oxides, ozone, and OH, Geophys. Res. Lett., 32, L09813, doi:10.1029/2005GL022469, 2005.

Fairlie, T. D., Jacob, D. J., and Park, R. J.: The impact of transpacific transport of mineral dust in the United States, Atmos. Environ., 41, 1251–1266, 2007.

Fisher, J. A., Jacob, D. J., Purdy, M. T., Kopacz, M., Le Sager, P., Carouge, C., Holmes, C. D., Yantosca, R. M., Batchelor, R. L., Strong, K., Diskin, G. S., Fuelberg, H. E., Holloway, J. S., Hyer, E. J., McMillan, W. W., Warner, J., Streets, D. G., Zhang, Q., Wang, Y., and Wu, S.: Source attribution and interannual variability of Arctic pollution in spring constrained by aircraft (ARCTAS, ARCPAC) and satellite (AIRS) observations of carbon monoxide, Atmos. Chem. Phys., 10, 977–996, doi:10.5194/acp-10-977-2010, 2010.

Fusco, A. C. and Logan, J. A.: Analysis of 1970–1995 trends in tropospheric ozone at Northern Hemisphere midlatitudes with the GEOS-CHEM model, J. Geophys. Res.-Atmos., 108, doi:10.1029/2002JD002742, 2003.

Guenther, A., Karl, T., Harley, P., Wiedinmyer, C., Palmer, P. I., and Geron, C.: Estimates of global terrestrial isoprene emissions using MEGAN (Model of Emissions of Gases and Aerosols from Nature), Atmos. Chem. Phys., 6, 3181–3210, doi:10.5194/acp-6-3181-2006, 2006.

Guicherit, R. and Roemer, M.: Tropospheric ozone trends, Chemosphere-Glob. Chang. Sci., 2, 167–183, 2000.

Helsel, D. R. and Hirsch, R. M.: Statistical methods in water resources, US Geological survey, Reston, Va., 2002.

Holloway, T., Hiram Levy, I., and Kasibhatla, P.: Global distribution of carbon monoxide, J. Geophys. Res., 105, 12123–12147, 2000.

Honrath, R. E., Owen, R. C., Val Martin, M., Reid, J. S., Lapina, K., Fialho, P., Dziobak, M. P., Kleissl, J., and Westphal, D. L.: Regional and hemispheric impacts of anthropogenic and

Title Page

Abstract | Introduction

Conclusions | References

Tables | Figures

|◄ | ►|

◄ | ►

Back | Close

Full Screen / Esc

Printer-friendly Version

Interactive Discussion

biomass burning emissions on summertime CO and O_3 in the North Atlantic lower free troposphere, J. Geophys. Res., 109, D24310, doi:10.1029/2004JD005147, 2004.

Hudman, R. C., Murray, L. T., Jacob, D. J., Turquety, S., Wu, S., Millet, D. B., Avery, M., Goldstein, A. H., and Holloway, J.: North American influence on tropospheric ozone and the effects of recent emission reductions: Constraints from ICARTT observations, J. Geophys. Res., 114, D07302, doi:10.1029/2008JD010126, 2009.

Jacob, D. J., Horowitz, L. W., Munger, J. W., Heikes, B. G., Dickerson, R. R., Artz, R. S., and Keene, W. C.: Seasonal transition from NO_x-to hydrocarbon-limited conditions for ozone production over the eastern United States in September, J. Geophys. Res., 100, 9315–9315, 1995.

Jaffe, D., Price, H., Parrish, D., Goldstein, A., and Harris, J.: Increasing background ozone during spring on the west coast of North America, Geophys. Res. Lett., 30, 1613, doi:10.1029/2003GL017024, 2003.

Johnson, C. E., Collins, W. J., Stevenson, D. S., and Derwent, R. G.: Relative roles of climate and emissions changes on future tropospheric oxidant concentrations, J. Geophys. Res., 104, 18631–18645, 1999.

Khalil, M. A. K. and Rasmussen, R. A.: Global decrease in atmospheric carbon monoxide, Nature, 370, 639–641, 1994.

Kleinman, L., Lee, Y. N., Springston, S. R., Lee, J. H., Nunnermacker, L., Weinstein-Lloyd, J., and Zhou, X.: Peroxy radical concentration and ozone formation rate, J. Geophys. Res., 100, 7263–7273, 1995.

Kleissl, J., Honrath, R. E., Dziobak, M. P., Tanner, D., Martin, M. V., Owen, R. C., and Helmig, D.: Occurrence of upslope flows at the Pico mountaintop observatory: A case study of orographic flows on a small, volcanic island, J. Geophys. Res., 112, 10, doi:10.1029/2006JD007565, 2007.

Kopacz, M., Jacob, D. J., Fisher, J. A., Logan, J. A., Zhang, L., Megretskaia, I. A., Yantosca, R. M., Singh, K., Henze, D. K., Burrows, J. P., Buchwitz, M., Khlystova, I., McMillan, W. W., Gille, J. C., Edwards, D. P., Eldering, A., Thouret, V., and Nedelec, P.: Global estimates of CO sources with high resolution by adjoint inversion of multiple satellite datasets (MOPITT, AIRS, SCIAMACHY, TES), Atmos. Chem. Phys., 10, 855–876, doi:10.5194/acp-10-855-2010, 2010.

Law, K.: Atmospheric chemistry: More ozone over North America, Nature, 463, 307–308, 2010.

Lee, S. H., Akimoto, H., Nakane, H., Kurnosenko, S., and Kinjo, Y.: Lower tropospheric ozone trend observed in 1989–1997 at Okinawa, Japan, Geophys. Res. Lett., 25, 1637–1640, 1998.

Lelieveld, J., Van Aardenne, J., Fischer, H., De Reus, M., Williams, J., and Winkler, P.: Increasing ozone over the Atlantic Ocean, Science, 304, 1483–1487, 2004.

Li, Q., Jacob, D. J., Bey, I., Palmer, P. I., Duncan, B. N., Field, B. D., Martin, R. V., Fiore, A. M., Yantosca, R. M., Parrish, D. D., Simmonds, P. G., and Oltmans, S. J.: Transatlantic transport of pollution and its effects on surface ozone in Europe and North America, J. Geophys. Res, 107, doi:10.1029/2001JD001422, 2002.

Martin, R. V., Chance, K., Jacob, D. J., Kurosu, T. P., Spurr, R. J. D., Bucsela, E., Gleason, J. F., Palmer, P. I., Bey, I., Fiore, A. M., Li, Q., Yantosca, R. M., and Koelemeijer, R. B. A.: An improved retrieval of tropospheric nitrogen dioxide from GOME, J. Geophys. Res., 107, 4437–4456, doi:10.1029/2001JD001027, 2002.

McLinden, C. A., Olsen, S. C., Hannegan, B., Wild, O., Prather, M. J., and Sundet, J.: Stratospheric ozone in 3-D models: A simple chemistry and the cross-tropopause flux, J. Geophys. Res., 105, 14653–14665, doi:10.1029/2000JD900124, 2000.

McMillan, W. W., Barnet, C., Strow, L., Chahine, M. T., McCourt, M. L., Novelli, P. C., Korontzi, S., Maddy, E. S., and Datta, S.: Daily global maps of carbon monoxide: First views from NASA's Atmospheric Infra-Red Sounder, Geophys. Res. Lett., 32, L11801, doi:10.1029/2004GL021821, 2005.

Olivier, J. G. J. and Berdowski, J. J. M.: Global emission sources and sinks, in: The Climate System, edited by: Berdowski, J., Guicherit, R., and Heij, B. J., Swets & Zeitlinger, Lisse, the Netherlands, 33–77, 2001.

Oltmans, S. J., Lefohn, A. S., Harris, J. M., Galbally, I., Scheel, H. E., Bodeker, G., Brunke, E., Claude, H., Tarasick, D., Johnson, B. J., Simmonds, P, Shadwick, D., Anlauf, K., Hayden, K., Schmidlin, F., Fujimoto, T., Akagi, K., Meyer, C., Nichol, S., Davies, J., Redondas, A., and Cuevas, E.: Long-term changes in tropospheric ozone, Atmos. Environ., 40, 3156–3173, 2006

Park, R. J., Jacob, D. J., Field, B. D., Yantosca, R. M., and Chin, M.: Natural and transboundary pollution influences on sulfate-nitrate-ammonium aerosols in the United States: Implications for policy, J. Geophys. Res., 109, D15204, doi:10.1029/2003JD004473, 2004.

Sandu, A. and Sander, R.: Technical note: Simulating chemical systems in Fortran90 and Matlab with the Kinetic PreProcessor KPP-2.1, Atmos. Chem. Phys., 6, 187–195, doi:10.5194/acp-6-187-2006, 2006.

Seinfeld, J. H. and Pandis, S. N.: Atmospheric Chemistry and Physics: From Air Pollution to Climate Change, John Wiley, New York, 2006.

Streets, D. G., Bond, T. C., Carmichael, G. R., Fernandes, S. D., Fu, Q., He, D., Klimont, Z., Nelson, S. M., Tsai, N. Y., Wang, M. Q., Woo, J. H., and Yarber, K. F.: An inventory of gaseous and primary aerosol emissions in Asia in the year 2000, J. Geophys. Res., 108, 8809, doi:10.1029/2002JD003093, 2003.

Streets, D. G., Zhang, Q., Wang, L., He, K., Hao, J., Wu, Y., Tang, Y., and Carmichael, G. R.: Revisiting China's CO emissions after the Transport and Chemical Evolution over the Pacific (TRACE-P) mission: synthesis of inventories, atmospheric modeling, and observations, J. Geophys. Res., 111, D14306, doi:10.1029/2006JD007118, 2006.

Val Martin, M., Honrath, R., Owen, R., Pfister, G., Fialho, P., and Barata, F.: Significant enhancements of nitrogen oxides, black carbon, and ozone in the North Atlantic lower free troposphere resulting from North American boreal wildfires, J. Geophys. Res, 111, D23S60, doi:10.1029/2006JD007530, 2006.

Val Martin, M., Honrath, R., Owen, R., and Lapina, K.: Large-scale impacts of anthropogenic pollution and boreal wildfires on the nitrogen oxides over the central North Atlantic region, J. Geophys. Res., 113, D17308, doi:10.1029/2007JD009689, 2008a.

Val Martin, M., Honrath, R., Owen, R., and Li, Q.: Seasonal variation of nitrogen oxides in the central North Atlantic lower free troposphere, J. Geophys. Res.-Atmos., 113, D17307, doi:10.1029/2007JD009688, 2008b.

van der Werf, G. R., Randerson, J. T., Giglio, L., Collatz, G. J., Kasibhatla, P. S., and Arellano Jr., A. F.: Interannual variability in global biomass burning emissions from 1997 to 2004, Atmos. Chem. Phys., 6, 3423–3441, doi:10.5194/acp-6-3423-2006, 2006.

van der Werf, G. R., Randerson, J. T., Giglio, L., Collatz, G. J., Mu, M., Kasibhatla, P. S., Morton, D. C., DeFries, R. S., Jin, Y., and van Leeuwen, T. T.: Global fire emissions and the contribution of deforestation, savanna, forest, agricultural, and peat fires (1997–2009), Atmos. Chem. Phys., 10, 11707–11735, doi:10.5194/acp-10-11707-2010, 2010.

Vingarzan, R.: A review of surface ozone background levels and trends, Atmos. Environ., 38, 3431–3442, 2004.

Title Page

Abstract | Introduction

Conclusions | References

Tables | Figures

Back | Close

Full Screen / Esc

Printer-friendly Version

Interactive Discussion

Wang, H., Jacob, D. J., Le Sager, P., Streets, D. G., Park, R. J., Gilliland, A. B., and Van Donke-laar, A.: Surface ozone background in the United States: Canadian and Mexican pollution influences, Atmos. Environ., 43, 1310–1319, 2009.

Wang, Y., Jacob, D. J., and Logan, J. A.: Global simulation of tropospheric O_3-NO^--hydrocarbon chemistry, 1. Model formulation, J. Geophys. Res., 103, 10713–10725, 1998.

Wu, S., Mickley, L. J., Jacob, D. J., Rind, D., and Streets, D. G.: Effects of 2000–2050 changes in climate and emissions on global tropospheric ozone and the policy-relevant background surface ozone in the United States, J. Geophys. Res.-Atmos., 113, doi:10.1029/2007JD009639, 2008.

Wu, S., Mickley, L. J., Jacob, D. J., Logan, J. A., Yantosca, R. M., and Rind, D.: Why are there large differences between models in global budgets of tropospheric ozone?, J. Geophys. Res., 112, D05302, doi:10.1029/2006JD007801, 2007.

Yurganov, L. N., McMillan, W. W., Dzhola, A. V., Grechko, E. I., Jones, N. B., and van der Werf, G. R.: Global AIRS and MOPITT CO measurements: validation, comparison, and links to biomass burning variations and carbon cycle, J. Geophys. Res.-Atmos., 113, 14, doi:10.1029/2007JD009229, 2008.

Zhang, L., Jacob, D. J., Liu, X., Logan, J. A., Chance, K., Eldering, A., and Bojkov, B. R.: Intercomparison methods for satellite measurements of atmospheric composition: application to tropospheric ozone from TES and OMI, Atmos. Chem. Phys., 10, 4725–4739, doi:10.5194/acp-10-4725-2010, 2010.

Zhang, Q., Streets, D. G., Carmichael, G. R., He, K. B., Huo, H., Kannari, A., Klimont, Z., Park, I. S., Reddy, S., Fu, J. S., Chen, D., Duan, L., Lei, Y., Wang, L. T., and Yao, Z. L.: Asian emissions in 2006 for the NASA INTEX-B mission, Atmos. Chem. Phys., 9, 5131–5153, doi:10.5194/acp-9-5131-2009, 2009.

Title Page

Abstract | Introduction

Conclusions | References

Tables | Figures

◀ | ▶|

◀ | ▶

Back | Close

Full Screen / Esc

Printer-friendly Version

Interactive Discussion

Table 1. Anthropogenic and biomass burning CO emissions used in GEOS-Chem (values are in $Tg\,CO\,yr^{-1}$).

Year	Anthropogenic				Biomass burning	
	Northern Hemisphere	North America	Europe	Asia	Northern Hemisphere	North America
2001	436.5	97.3	45.1	245.9	202.6	8.7
2002	447.9	99.9	42.8	256.0	230.9	21.3
2003	460.3	95.5	41.6	272.9	246.5	33.9
2004	461.1	90.6	41.6	278.1	201.0	23.2
2005	460.1	86.3	40.0	281.8	216.0	20.7
2006	460.7	83.0	38.2	286.2	180.9	15.5
2007	455.9	83.0	35.4	286.2	219.6	15.3
2008	457.2	83.2	35.6	287.0	180.9	13.8
2009	455.9	83.0	35.4	286.2	180.0	13.8

Title Page

Abstract | Introduction

Conclusions | References

Tables | Figures

◀◀ | ▶▶

◀ | ▶

Back | Close

Full Screen / Esc

Printer-friendly Version

Interactive Discussion

Table 2. CO and O_3 trends obtained for PMO observations and GEOS-Chem output.

Species	Trend (ppbv yr^{-1})*		P value	
	Observations	GEOS-Chem	Observations	GEOS-Chem
CO	-0.31 ± 0.30	-0.34 ± 0.08	0.04	< 0.001
O_3	-0.21 ± 0.11	-0.53 ± 0.04	< 0.001	< 0.001

* Uncertainties are in the 2-σ (95 %) interval.

Table 3. GEOS-Chem North American fossil fuel emissions contribution to mixing ratios of CO and O_3 at PMO (means for every season from fall 2000 to summer 2010).

Season	CO (ppbv)	O_3 (ppbv)
Fall	5.7	4.4
Winter	12.7	2.3
Spring	11.0	4.5
Summer	4.9	4.9
Annual	8.6	4.0

Table 4. Trends in contributions to CO at PMO from various regions and sources[a].

CO source[b]	Trend (ppbv yr^{-1})[c]	P value
CO (ff USA)	-0.27 ± 0.05	< 0.001
CO (ff Europe)	-0.004 ± 0.03	0.39
CO (ff Asia)	$+0.35 \pm 0.03$	< 0.001
CO (bb North America)	-0.03 ± 0.02	0.004
CO (bb Europe)	-0.30 ± 0.03	< 0.001
CO (bb Asia)	$+0.05 \pm 0.01$	< 0.001

[a] Results based on GEOS-Chem tagged CO simulation results.
[b] ff = emissions from fossil fuel combustion; bb = emissions from biomass burning.
[c] Uncertainties are in the 2-σ (95 %) interval.

|◄ | ►|

◄ | ►

Back | Close

Full Screen / Esc

Printer-friendly Version

Interactive Discussion

Table 5. Trends in contributions to O_3 at PMO from various regions and sources[a].

O_3 source[b]	Trend (ppbv yr^{-1})[c]	P value
O_3 (produced over the USA)	-0.18 ± 0.03	< 0.001
O_3 (produced in the NA BL)	-0.57 ± 0.02	< 0.001
O_3 (produced in the Asian BL)	-0.12 ± 0.004	< 0.001
O_3 (produced in the European BL)	-0.09 ± 0.003	< 0.001
O_3 (produced in the NAtl BL)	-0.51 ± 0.02	< 0.001
O_3 (produced in the UT)	$+3.13 \pm 0.07$	< 0.001
O_3 (produced in the MT)	-2.19 ± 0.05	< 0.001

[a] Results based on GEOS-Chem tagged O_3 simulation results.
[b] NA: North America, BL: Boundary Layer, NAtl: North Atlantic, UT: Upper Troposphere, MT: Middle Troposphere.
[c] Uncertainties are in the 2-σ (95 %) interval.

U.S. Emission Trends (2000-2011)

CO = 7305.66-(3.601*Time)
R² = 0.97

NOx = 1448.19 -(0.714*Time)
R² = 0.98
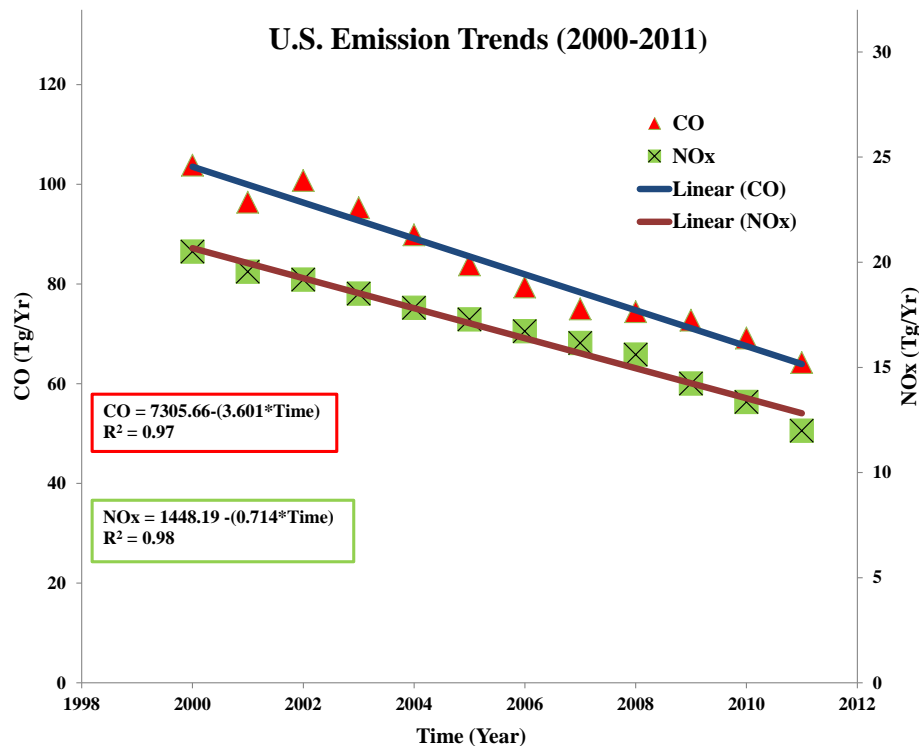
Fig. 1. US anthropogenic emissions (in $Tg\,yr^{-1}$) for CO and NO_x from 2000 to 2011. (Data available at: http://www.epa.gov/ttnchie1/trends/).
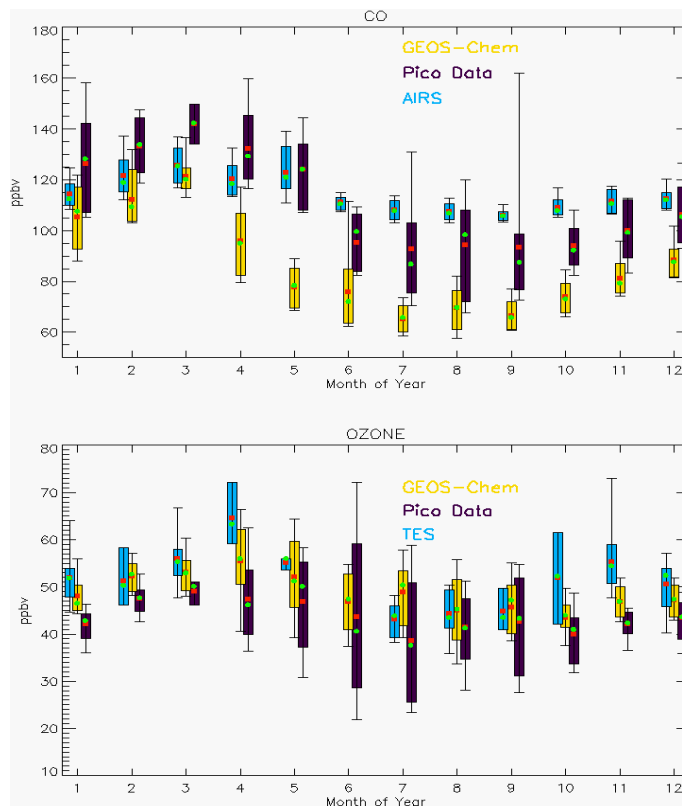
Fig. 2. Seasonal variation of CO (top) and O$_3$ (bottom) at PMO (September 2004–August 2005). GEOS-Chem model simulations (yellow), in-situ measurements (dark brown) and satellite observations (AIRS for CO and TES for O$_3$) (light blue). The thick (thin) bars represent the 67 % (90 %) confidence intervals. The mean and median are represented with red and green dots respectively. The statistics are based on daily (24 h) averages.
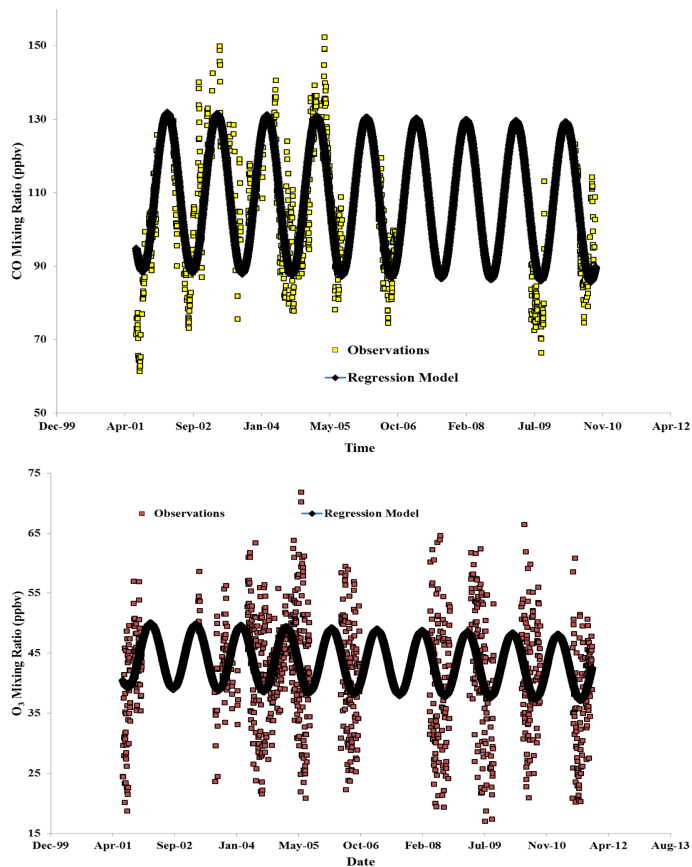
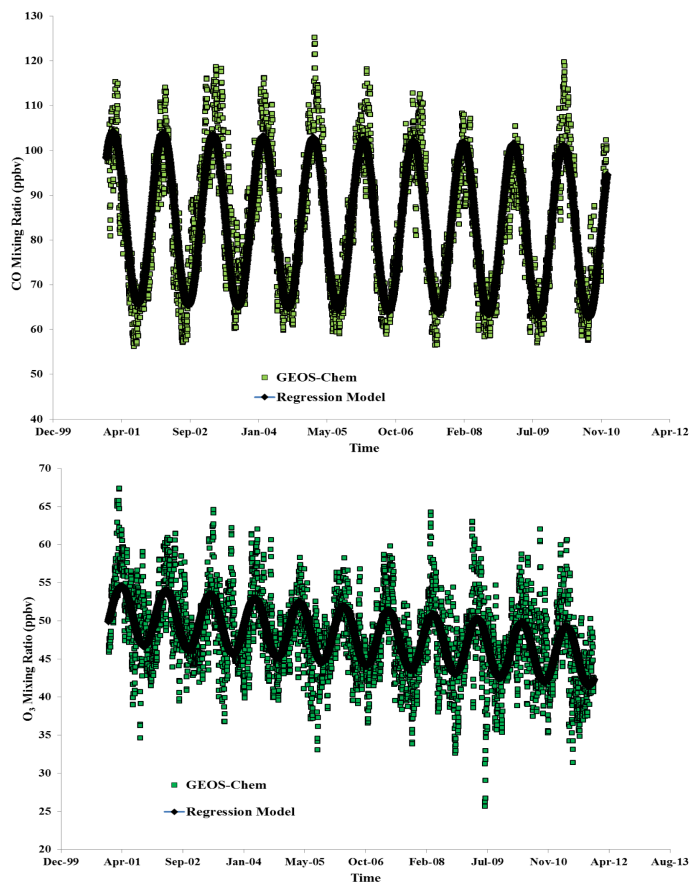**Fig. 3.** Regression model fit to the PMO observations for CO (top) and O$_3$ (bottom).

Fig. 4. Regression model fit to the GEOS-Chem (full chemistry simulation with normal emissions) output for CO (top) and O_3 (bottom) at PMO.